Acta Crystallographica Section F
Structural Biology and Crystallization Communications
ISSN 1744-3091

The macromolecular complex of ICP and falcipain-2 from *Plasmodium*: preparation, crystallization and preliminary X-ray diffraction analysis

Guido Hansen,[a] Britta Schwarzloh,[a] Annika Rennenberg,[b] Volker T. Heussler[b,c] and Rolf Hilgenfeld[a,d,e]*

[a]Institute of Biochemistry, Center for Structural and Cell Biology in Medicine, University of Lübeck, Ratzeburger Allee 160, 23538 Lübeck, Germany, [b]Bernhard Nocht Institute for Tropical Medicine, Bernard-Nocht-Strasse 74, 20359 Hamburg, Germany, [c]Institute of Cell Biology, University of Bern, Baltzerstrasse 4, 3012 Bern, Switzerland, [d]Shanghai Institute of Materia Medica, Chinese Academy of Sciences, 555 Zu Chong Zhi Road, Shanghai 201203, People's Republic of China, and [e]Laboratory for Structural Biology of Infection, c/o DESY, Building 22a, Notkestrasse 85, 22603 Hamburg, Germany

Correspondence e-mail: hilgenfeld@biochem.uni-luebeck.de

Received 16 July 2011
Accepted 22 August 2011

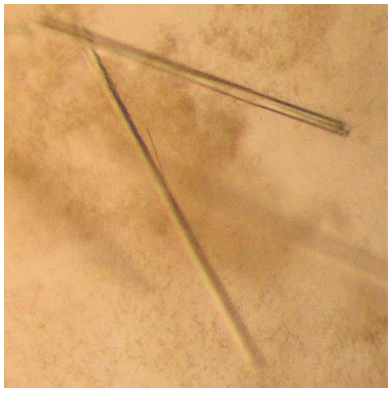

The malaria parasite *Plasmodium* depends on the tight control of cysteine-protease activity throughout its life cycle. Recently, the characterization of a new class of potent inhibitors of cysteine proteases (ICPs) secreted by *Plasmodium* has been reported. Here, the recombinant production, purification and crystallization of the inhibitory C-terminal domain of ICP from *P. berghei* in complex with the *P. falciparum* haemoglobinase falcipain-2 is described. The 1:1 complex was crystallized in space group $P4_3$, with unit-cell parameters $a = b = 71.15$, $c = 120.09$ Å. A complete diffraction data set was collected to a resolution of 2.6 Å.

1. Introduction

Facilitating uptake and egress from host cells, activation of pro-enzymes and haemoglobin degradation, cysteine proteases have important functions during most stages of the complex life cycle of the malaria parasite *Plasmodium* (Coppens *et al.*, 2010; Drew *et al.*, 2008; Hogg *et al.*, 2006; Rosenthal, 2004; Sturm *et al.*, 2006). Especially well characterized is the role of *Plasmodium* cysteine proteases in haemoglobin hydrolysis, which takes place during the blood stage after uptake of parasites into erythrocytes. Previously, we and others have determined the structure of the papain-type protease falcipain-2 (FP-2), which is critical for intraerythrocytic haemoglobin breakdown (Wang *et al.*, 2006; Hogg *et al.*, 2006; Kerr *et al.*, 2009). *Plasmodium* tightly controls the proteolytic activity of FPs and other endogenous cysteine proteases, and stage-specific activation is vital for survival and successful propagation of the parasite within its host. It has been suggested that in addition to its own proteases, *Plasmodium* regulates the activity of host-cell cysteine proteases (Pandey *et al.*, 2006), which mediate apoptosis and represent an important part of the host's immune system through presentation of parasite-derived material by MHC molecules. Many organisms employ specific protease inhibitors to shut down proteases at times when proteolytic activity might be harmful.

The genomes of *Plasmodium* species encode an endogenous protease inhibitor belonging to the recently defined family of inhibitors of cysteine proteases (ICPs; MEROPS family I42; Rawlings *et al.*, 2008). In *P. falciparum*, ICP has been designated as falstatin (Pandey *et al.*, 2006). ICP proteins have also been identified in other eukaryotes, bacteria and archaea (Rigden *et al.*, 2002; Sanderson *et al.*, 2003). While chagasin, a member of the I42 family, regulates the activity of the endogenous protease cruzipain in *Trypanosoma cruzi* (Monteiro *et al.*, 2001), the target proteases for other ICPs are largely unknown (Sanderson *et al.*, 2003). To date, only two members of the I42 family have been structurally characterized. The structures of chagasin and ICP from *Leishmania mexicana* have been determined by X-ray crystallography (Figueiredo da Silva *et al.*, 2007) and NMR (Salmon *et al.*, 2006; Smith *et al.*, 2006). In addition, X-ray structures of macromolecular complexes of cysteine proteases with chagasin are

available, showing that the inhibitor interacts with target proteases *via* a tripartite binding motif that includes loops L2, L4 and L6 (Ljunggren *et al.*, 2007; Redzynia *et al.*, 2008, 2009; Wang *et al.*, 2007).

Plasmodium ICPs consist of a chagasin-like C-terminal part (ICP-C) and a unique nonhomologous N-terminal part (ICP-N) of unknown function which is missing in other ICP-family members. The C-terminal domain of *Plasmodium* ICPs acts as a potent inhibitor of FP-2 and other cysteine proteases (Hansen *et al.*, 2011; Rennenberg *et al.*, 2010). However, the structure, function and target protease(s) of *Plasmodium* ICPs are largely unknown. Here, we report the production, purification and crystallization of ICP-C from *P. berghei* (PbICP-C) in complex with FP-2. The three-dimensional structure determination will enable an in-depth understanding of *Plasmodium* ICPs and provide detailed information on specific interactions with target proteases.

2. Cloning

A plasmid for the expression of PbICP-C was constructed by amplifying the DNA sequence encoding amino-acid residues 190–354 from cDNA using 5′-TT**CATATG**GGAGATGAAAAATGTGGTAAATCA-3′ as the forward primer and 5′-TT**GAATTC**TTATTGGACAGTCACGTATATAAT-3′ as the reverse primer, including *Nde*I and *Eco*RI restriction sites (bold), respectively. The PCR product was purified and ligated into a pJC45 expression vector (Schlüter *et al.*, 2000) encoding an N-terminal His_{10} tag. After verification of the DNA sequence, the plasmid was transformed into BL21 (DE3) competent cells harbouring a pAPlacI^{Q} plasmid (Schlüter *et al.*, 2000). The cloning of FP-2 (FP-2 Cys42Ala, a mature inactive variant of the FP-2 precursor, previously designated FPc285aM) has been described elsewhere (Hogg *et al.*, 2006). The complete amino-acid sequences of PbICP-C and FP-2 are given in Appendix *A*.

3. Protein production and purification and preparation of the PbICP-C–FP-2 complex

Recombinant PbICP-C was expressed at 310 K by the addition of isopropyl *β*-D-1-thiogalactopyranoside (IPTG; final concentration 1 m*M*; Biomol) to 6 l *Escherichia coli* cultures at OD_{600} = 0.7–0.9. After 2 h, cells were harvested by centrifugation (3000*g*, 277 K, 15 min) and stored at 253 K. Cell pellets were resuspended in 50 ml 50 m*M* NaH_2PO_4, 300 m*M* NaCl, 10 m*M* imidazole, pH 8.0, and the cells were lysed by sonication. After centrifugation (10 000*g*, 277 K, 30 min), the supernatant was mixed with 3.6 ml of a 50%(*v*/*v*) slurry of Ni–NTA resin (Qiagen) and incubated for 1 h at 277 K. The suspension was transferred to an empty propylene column (Qiagen) and the purification continued at room temperature. The column was washed with 200 ml 50 m*M* NaH_2PO_4, 300 m*M* NaCl, 20 m*M* imidazole, pH 8.0, followed by a high-salt washing step with 200 ml 50 m*M* NaH_2PO_4, 2 *M* NaCl, 50 m*M* imidazole, pH 8.0, and subsequently washed again with 100 ml 50 m*M* NaH_2PO_4, 300 m*M* NaCl, 20 m*M* imidazole, pH 8.0. Bound protein was eluted with 50 m*M* NaH_2PO_4, 300 m*M* NaCl, 250 m*M* imidazole, pH 8.0. After SDS–PAGE analysis, fractions containing PbICP-C were pooled and concentrated to 6 mg ml^{-1} and the buffer was exchanged to 500 m*M* NaCl, 20 m*M* Tris, pH 7.5 using centrifugal concentrators (Sartorius). Purified PbICP-C was stored at 277 K.

Inactive mature FP-2 was recombinantly produced and purified in *E. coli* Origami (DE3) (Novagen). Cells were transformed with the corresponding plasmid and a 4 l culture was grown at 310 K to OD_{600} = 0.6. Expression was induced by the addition of IPTG to a final concentration of 0.5 m*M*. After 4 h incubation, cells were harvested by centrifugation (5000*g*, 277 K, 15 min) and stored at 253 K. Cell pellets were resuspended in 40 ml 50 m*M* Tris, 1 m*M* EDTA, pH 7.5, and lysed by sonication. As FP-2 was produced as inclusion bodies, the supernatant was removed after centrifugation (27 000*g*, 277 K, 30 min). Protein purity was improved by washing the inclusion bodies twice with 20 ml buffer *A* (2 *M* urea, 2.5% Triton X-100, 20 m*M* Tris, pH 8.0) and twice with 20 ml buffer *B* (20% sucrose, 20 m*M* Tris, pH 8.0). Inclusion bodies were resuspended by sonication and pelleted by centrifugation (27 000*g*, 277 K, 30 min) after each washing step. To remove DNA, the pellet was resuspended in 5 ml buffer *B* containing 125 units of Benzonase (Sigma) and 10 m*M* $MgCl_2$ and stirred overnight at 277 K. 25 ml buffer *B* was added and the inclusion bodies were pelleted (27 000*g*, 277 K, 30 min) before solubilization in 15 ml denaturing buffer (8 *M* urea, 1 *M* imidazole, 20 m*M* Tris, pH 8.0). After 120 min incubation at room temperature, insoluble material was removed by centrifugation (27 000*g*, 277 K, 30 min) and FP-2 was refolded by rapid dilution (1:50) in refolding buffer (25 m*M* CAPS, 20% sucrose, 250 m*M* L-arginine, 1 m*M* EDTA, 1 m*M* reduced glutathione, 0.5 m*M* glutathione disulfide, pH 9.5). After incubation at 277 K for 20 h, the pH was adjusted to 7.5 by the addition of acetic acid and precipitated protein was removed by filtration (0.22 µm). The volume of the

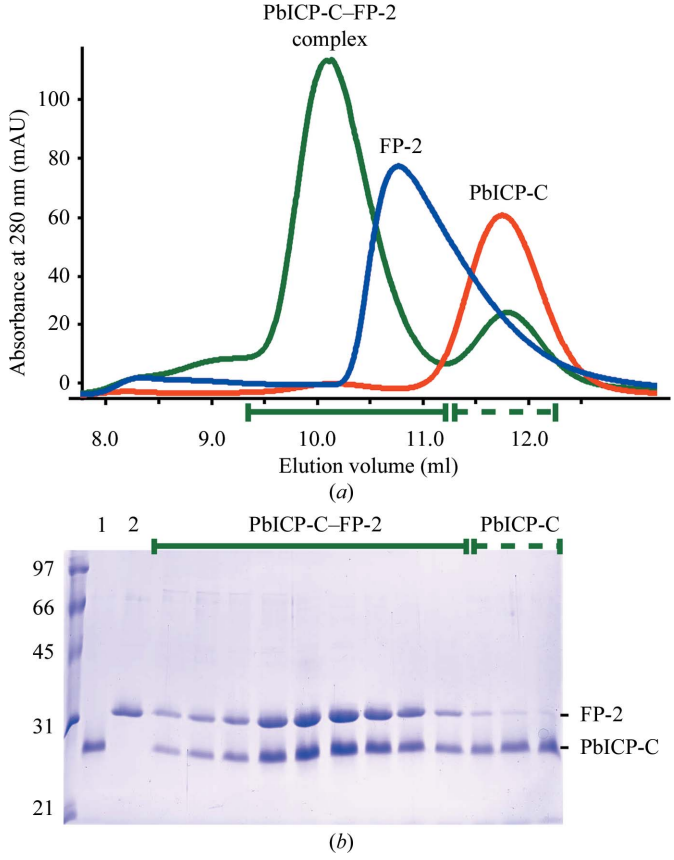

Figure 1
Isolation of the PbICP-C–FP-2 complex by SEC. (*a*) SEC elution profiles of PbICP-C (red), FP-2 (blue) and a sample after incubation of both proteins (green). The samples of purified PbICP-C or FP-2 eluted at the volumes expected for monomeric species (PbICP-C, 11.75 ml, 23.6 kDa; FP-2, 10.77 ml, 36.9 kDa). The elution volume of the pre-incubated sample containing both proteins corresponds to the formation of a 1:1 complex between FP-2 and PbICP-C (10.13 ml, 49.3 kDa). (*b*) SDS–PAGE analysis of purified PbICP-C (lane 1), FP-2 (lane 2) and fractions after SEC confirming the formation of the PbICP-C–FP-2 complex (indicated by green bars above the gel).

protein solution was reduced to 40 ml using a 400 ml stirred ultrafiltration cell (Amicon) and it was dialysed overnight against buffer *C* (50 m*M* NaCl, 20 m*M* Tris, pH 7.5, 277 K), loaded onto a 5 ml HiTrap Q HP anion-exchange column (GE Healthcare) and eluted with a linear gradient of 50 m*M* to 1 *M* NaCl at room temperature. After SDS–PAGE analysis, fractions containing FP-2 were pooled, concentrated to 2 mg ml^{-1} using centrifugal concentrators (Sartorius) and stored at 277 K.

Purified proteins were analysed by size-exclusion chromatography (SEC) at room temperature using a Superdex 75 column (10 × 300 mm; GE Healthcare) equilibrated with buffer *D* (500 m*M* NaCl, 20 m*M* Tris, pH 7.5). The elution profiles (280 nm) of PbICP-C and FP-2 showed single symmetric peaks at elution volumes indicating that both proteins exist as monomers in solution (PbICP-C, 11.75 ml, 23.6 kDa; FP-2, 10.77 ml, 36.9 kDa; Fig. 1*a*). To allow the formation of protease–inhibitor complexes, PbICP-C and FP-2 were mixed to final concentrations of 1 mg ml^{-1} each in buffer *D* and incubated overnight at 277 K. The SEC elution profile of the sample showed a peak at 11.8 ml (23.1 kDa) and a higher molecular-weight peak at 10.13 ml (49.3 kDa; Fig. 1*a*). SDS–PAGE analysis confirmed that the higher molecular-weight species consisted of PbICP-C and FP-2 in a stoichiometric ratio, indicating the formation of a 1:1 complex, whereas the lower molecular-weight species originated from excess free PbICP-C (Fig. 1*b*). For preparative isolation of the PbICP-C–FP-2 complex, a Superdex 75 column (16 × 600 mm; GE Healthcare) at room temperature was used; fractions containing the complex were pooled, concentrated to 2 mg ml^{-1} using centrifugal concentrators (Sartorius) and stored at 277 K. The isolated complex was highly stable even after several months of storage as confirmed by SDS–PAGE and analytical SEC.

4. Crystallization

Initial crystallization screening was performed at 293 K using the sitting-drop vapor-diffusion technique in 96-well Intelli-Plates (Dunn Laboratories) with commercial and in-house sparse-matrix screening solutions. Subsequent optimization of conditions promoting crystal growth was performed in 24-well Cryschem plates (Hampton Research) by mixing 1 µl protein complex solution (2 mg ml^{-1} protein in buffer *D*) and 1 µl reservoir solution. SDS–PAGE analysis of dissolved crystals confirmed the presence of both PbICP-C and FP-2 (data not shown). Prior to diffraction experiments, crystals were directly transferred into reservoir solution supplemented with 30%(*v*/*v*) glycerol, mounted in CryoLoops (Hampton Research) and flash-cooled in liquid nitrogen. Although a number of crystals could

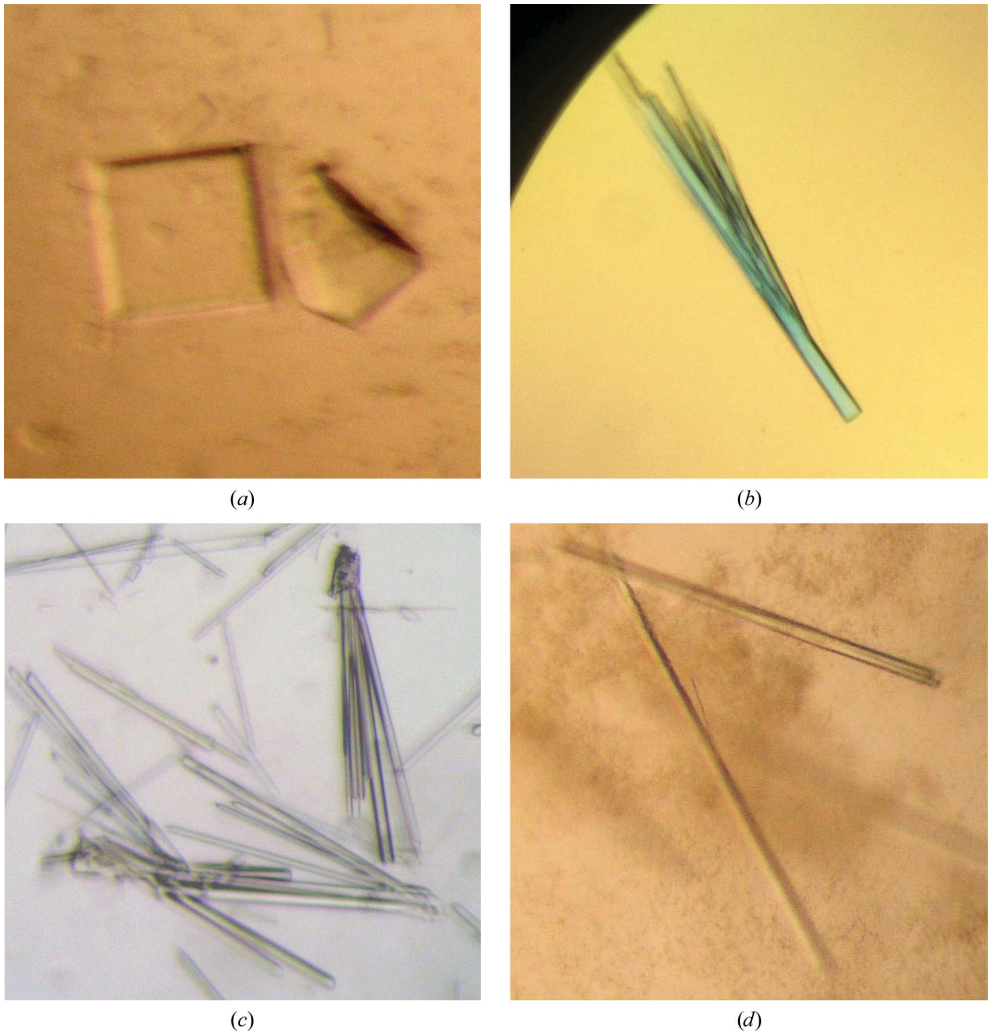

Figure 2
Crystals of PbICP-C–FP-2. (*a*)–(*c*) Typical crystals with poor diffraction properties grown without $CdCl_2$. (*d*) Well diffracting rod-like crystals grown in the presence of $CdCl_2$ [200 m*M* sodium acetate, 27.5 m*M* $CdCl_2$ and 100 m*M* MES (pH 5.0)]. Crystals grew within 2–4 weeks to final dimensions of 0.5 × 0.05 × 0.05 mm.

Table 1
Sample information.

Macromolecule details	
Database code(s)	PDB code 3pnr; unp codes q4yw59_plabe, q9n6s8_plafa
Component molecules	Falcipain-2 (mutation: C285A), PbICP-C, glycerol, cadmium ion, water
Macromolecular assembly	1:1 complex of PbICP-C and FP-2
Mass (Da)	48184.3
Source organism	Falcipain-2, *Plasmodium falciparum*; PbICP-C, *P. berghei*
Crystallization and crystal data	
Crystallization method	Vapor diffusion, sitting drop
Temperature (K)	291
Crystallization solutions	
Macromolecule	2 mg ml^{-1} PbICP-C–FP-2, 500 m*M* NaCl, 20 m*M* Tris pH 7.5
Reservoir	200 m*M* sodium acetate, 27.5 m*M* $CdCl_2$, 100 m*M* MES (pH 5.0)
Cryo treatment	
Final cryoprotection solution	140 m*M* sodium acetate, 19.25 m*M* $CdCl_2$, 70 m*M* MES (pH 5.0), 30%(*v*/*v*) glycerol
Crystal data	
Crystal size (mm)	0.5 × 0.05 × 0.05
Matthews coefficient, V_M (Å^3 Da^{-1})	3.16
Solvent content (%)	61
Unit-cell data	
Space group	$P4_3$
Unit-cell parameters (Å)	$a = b = 71.15$, $c = 120.09$
No. of protease–inhibitor complexes in unit cell, *Z*	1

Table 2
Data-collection statistics.

Values in parentheses are for the outer shell.

Diffraction source	Synchrotron; BESSY II beamline BL14.1
Diffraction protocol	Single wavelength
Monochromator	Double-crystal monochromator, Si(111)
Wavelength (Å)	0.9184
Detector	MAR mosaic 225 mm CCD
Temperature (K)	100
Resolution range (Å)	34.89–2.60 (2.74–2.60)
No. of observed reflections	17570 (2640)
Completeness (%)	95.2 (96.6)
Multiplicity	4.2 (4.1)
$\langle I/\sigma(I)\rangle$	8.1 (2.5)
R_{merge}†	0.10 (0.51)
$R_{p.i.m.}$‡	0.052 (0.283)
Data-processing software	*MOSFLM*; *SCALA*

† $R_{merge} = \sum_{hkl}\sum_i |I_i(hkl) - \langle I(hkl)\rangle| / \sum_{hkl}\sum_i I_i(hkl)$, where $I(hkl)$ is the intensity of reflection hkl and $\langle I(hkl)\rangle$ is the average intensity over all equivalent reflections. ‡ $R_{p.i.m.}$ is the precision-indicating merging R factor (Weiss & Hilgenfeld, 1997).

initially be obtained from different crystallization conditions, even after extensive optimization none of these crystals diffracted X-rays beyond 6 Å resolution using synchrotron-radiation sources (Figs. 2*a*–2*c*). Interestingly, crystals grown in the presence of Cd^{2+} showed greatly improved diffraction properties. Positive effects of Cd^{2+} ions on the crystallization of proteins have been reported previously (Trakhanov *et al.*, 1998; Trakhanov & Quiocho, 1995). In many cases, Cd^{2+}-mediated interactions stabilize intermolecular contacts of adjacent molecules in the crystal lattice (Trakhanov *et al.*, 1998). The best crystals of the PbICP-C–FP-2 complex were obtained using 200 m*M* sodium acetate, 27.5 m*M* $CdCl_2$ and 100 m*M* MES pH 5.0 as the reservoir solution. Rod-like crystals grew within 2–4 weeks to final dimensions of 0.5 × 0.05 × 0.05 mm (Fig. 2*d*). Details of samples and crystallization are summarized in Table 1.

5. X-ray data collection and preliminary X-ray analysis

X-ray diffraction data for several crystal forms from different crystallization conditions were collected using synchrotron radiation on beamline BL14.1, BESSY (Berlin, Germany), on beamline X13 (University of Hamburg–University of Lübeck–EMBL) at the DORIS storage ring, DESY (Hamburg, Germany) and on beamline I911, MAX-lab (Lund, Sweden). Diffraction data were processed, reduced and scaled with *MOSFLM* (Leslie, 1992) and *SCALA* (Evans, 2006). The best data set was collected to a resolution of 2.6 Å at 100 K from a single crystal at BESSY using a MAR mosaic 225 mm

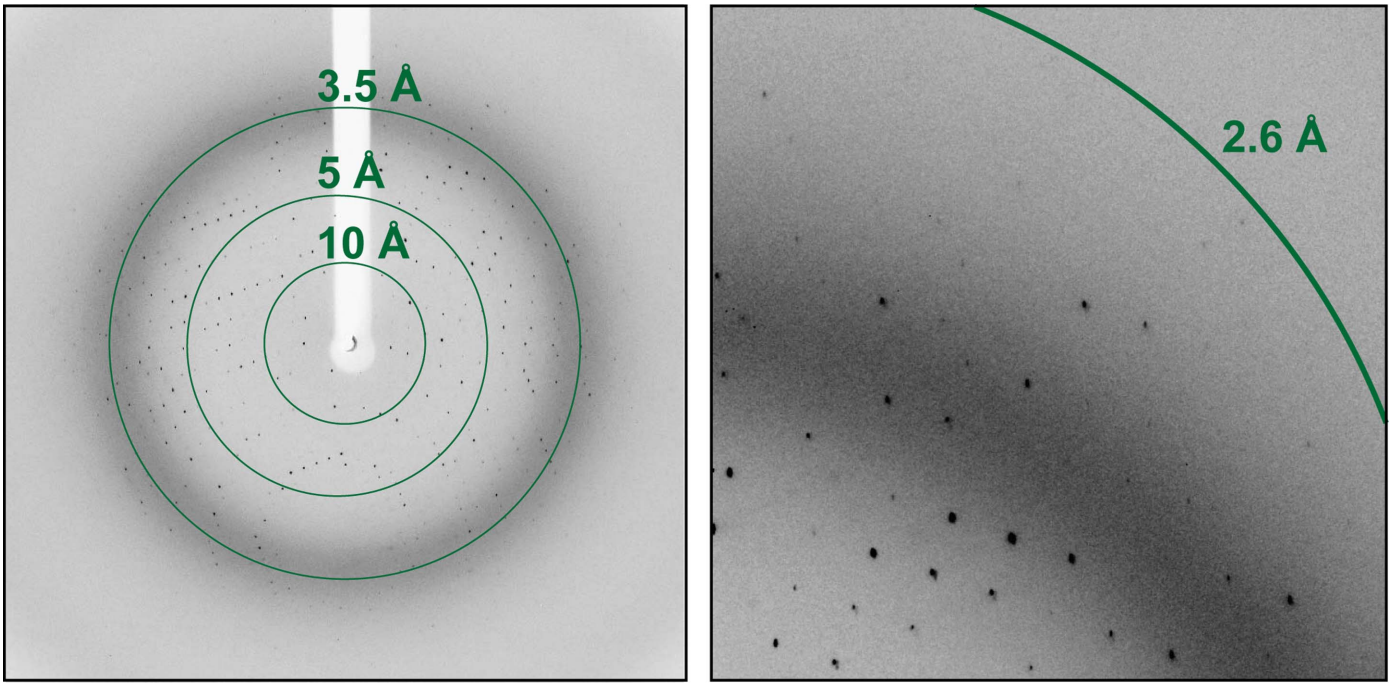

Figure 3
X-ray diffraction pattern at a resolution of 2.6 Å collected with 0.5° oscillation per image on beamline BL14.1 at BESSY (Berlin, Germany); circles indicate resolution shells.

CCD detector (Fig. 3). The crystals belonged to space group $P4_3$, with unit-cell parameters $a = b = 71.15$, $c = 120.09$ Å. Data-collection statistics are given in Table 2. The asymmetric unit contained one PbICP-C–FP-2 complex, corresponding to a Matthews coefficient (Matthews, 1968) of 3.16 Å^3 Da^{-1} and an estimated solvent content of 61%. Inspection of the asymmetric unit after molecular replacement [*Phaser Z* score of 19.5 (Storoni *et al.*, 2004); $R = 0.335$, $R_{free} = 0.373$ after initial refinement with *REFMAC* (Murshudov *et al.*, 2011)] using FP-2 as a search model (PDB entry 2ghu, chain *A*, residues 1–241; Hogg *et al.*, 2006) showed additional electron density that could be unambiguously attributed to a PbICP-C molecule. Full structure determination, refinement and analysis of the PbICP-C–FP-2 complex has been reported elsewhere (Hansen *et al.*, 2011).

APPENDIX *A*
Amino-acid sequences of crystallized components

A1. Amino-acid sequence of PbICP-C

MGHHHHHHHHHHSSGHIEGRHMGDEKCGKSLKLGNISNQTNQETITQSLSVGEILCIDLEGNAGTGYLWVLLGIHKDEPIINPENFPTKLTKKSFFSEEISVTQPKKYKIDEHDSSKNVNREIESPEQKESDSKPKKPQMQLLGGPDRMRSVIKGHKPGKYYIVYSYYRPFSPTSGANTKIIYVTVQ.

A2. Amino-acid sequence of FP-2

MNYEEVIKKYRGEENFDHAAYDWRLHSGVTPVKDQKNCGSAWAFSSIGSVESQYAIRKNKLITLSEQELVDCSFKNYGCNGGLINNAFEDMIELGGICPDGDYPYVSDAPNLCNIDRCTEKYGIKNYLSVPDNKLKEALRFLGPISISVAVSDDFAFYKEGIFDGECGDQLNHAVMLVGFGMKEIVNPLTKKGEKHYYYIIKNSWGQQWGERGFINIETDESGLMRKCGLGTDAFIPLIE.

This paper is dedicated to the memory of Anastância Joaquim, who died of misdiagnosed malaria on 9 July 2006. We thank S. Schmidtke for expert technical assistance and T. Ursby (MAX-lab, Lund, Sweden) as well as R. Wrase for assistance with synchrotron data collection. We acknowledge access to beamline BL14.1 of the BESSY II storage ring (Berlin, Germany) *via* the Joint Berlin MX-Laboratory sponsored by the Helmholtz Zentrum Berlin für Materialien und Energie, the Freie Universität Berlin, the Humboldt-Universität zu Berlin, the Max-Delbrück Centrum and the Leibniz-Institut für Molekulare Pharmakologie. Financial support by the DFG (Hi 611/5-1) is gratefully acknowledged. Experiments at MAX-lab were supported by the Integrated Infrastructure Initiative 'Integrating Activity on Synchrotron and Free Electron Laser Science' of the European Commission (EC), contract R II 3-CT-2004-506008. Optimization of PbICP-C–FP-2 crystals was performed within the OptiCryst project of the EC (LSH-2005-037793; http://www.opticryst.org). RH is supported by a Chinese Academy of Sciences Visiting Professorship for Senior International Scientists, grant No. 2010T1S6, by the DFG Cluster of Excellence 'Inflammation at Interfaces' (EXC 306) and by the Fonds der Chemischen Industrie. VTH is supported by the DFG through SFB 841 and by the MALSIG Consortium of the EC.

References

Coppens, I., Sullivan, D. J. & Prigge, S. T. (2010). *Trends Parasitol.* **26**, 305–310.
Drew, M. E., Banerjee, R., Uffman, E. W., Gilbertson, S., Rosenthal, P. J. & Goldberg, D. E. (2008). *J. Biol. Chem.* **283**, 12870–12876.
Evans, P. (2006). *Acta Cryst.* D**62**, 72–82.
Figueiredo da Silva, A. A., de Carvalho Vieira, L., Krieger, M. A., Goldenberg, S., Zanchin, N. I. & Guimarães, B. G. (2007). *J. Struct. Biol.* **157**, 416–423.
Hansen, G., Heitmann, A., Witt, T., Li, H., Jiang, H., Shen, X., Heussler, V. T., Rennenberg, A. & Hilgenfeld, R. (2011). *Structure*, **19**, 919–929.
Hogg, T., Nagarajan, K., Herzberg, S., Chen, L., Shen, X., Jiang, H., Wecke, M., Blohmke, C., Hilgenfeld, R. & Schmidt, C. L. (2006). *J. Biol. Chem.* **281**, 25425–25437.
Kerr, I. D., Lee, J. H., Pandey, K. C., Harrison, A., Sajid, M., Rosenthal, P. J. & Brinen, L. S. (2009). *J. Med. Chem.* **52**, 852–857.
Leslie, A. G. W. (1992). *Jnt CCP4/ESF–EACBM Newsl. Protein Crystallogr.* **26**.
Ljunggren, A., Redzynia, I., Alvarez-Fernandez, M., Abrahamson, M., Mort, J. S., Krupa, J. C., Jaskolski, M. & Bujacz, G. (2007). *J. Mol. Biol.* **371**, 137–153.
Matthews, B. W. (1968). *J. Mol. Biol.* **33**, 491–497.
Monteiro, A. C., Abrahamson, M., Lima, A. P., Vannier-Santos, M. A. & Scharfstein, J. (2001). *J. Cell Sci.* **114**, 3933–3942.
Murshudov, G. N., Skubák, P., Lebedev, A. A., Pannu, N. S., Steiner, R. A., Nicholls, R. A., Winn, M. D., Long, F. & Vagin, A. A. (2011). *Acta Cryst.* D**67**, 355–367.
Pandey, K. C., Singh, N., Arastu-Kapur, S., Bogyo, M. & Rosenthal, P. J. (2006). *PLoS Pathog.* **2**, e117.
Rawlings, N. D., Morton, F. R., Kok, C. Y., Kong, J. & Barrett, A. J. (2008). *Nucleic Acids Res.* **36**, D320–D325.
Redzynia, I., Ljunggren, A., Abrahamson, M., Mort, J. S., Krupa, J. C., Jaskolski, M. & Bujacz, G. (2008). *J. Biol. Chem.* **283**, 22815–22825.
Redzynia, I., Ljunggren, A., Bujacz, A., Abrahamson, M., Jaskolski, M. & Bujacz, G. (2009). *FEBS J.* **276**, 793–806.
Rennenberg, A., Lehmann, C., Heitmann, A., Witt, T., Hansen, G., Nagarajan, K., Deschermeier, C., Turk, V., Hilgenfeld, R. & Heussler, V. T. (2010). *PLoS Pathog.* **6**, e1000825.
Rigden, D. J., Mosolov, V. V. & Galperin, M. Y. (2002). *Protein Sci.* **11**, 1971–1977.
Rosenthal, P. J. (2004). *Int. J. Parasitol.* **34**, 1489–1499.
Salmon, D., do Aido-Machado, R., Diehl, A., Leidert, M., Schmetzer, O., de A. Lima, A. P. C., Scharfstein, J., Oschkinat, H. & Pires, J. R. (2006). *J. Mol. Biol.* **357**, 1511–1521.
Sanderson, S. J., Westrop, G. D., Scharfstein, J., Mottram, J. C. & Coombs, G. H. (2003). *FEBS Lett.* **542**, 12–16.
Schlüter, A., Wiesgigl, M., Hoyer, C., Fleischer, S., Klaholz, L., Schmetz, C. & Clos, J. (2000). *Biochim. Biophys. Acta*, **1491**, 65–74.
Smith, B. O., Picken, N. C., Westrop, G. D., Bromek, K., Mottram, J. C. & Coombs, G. H. (2006). *J. Biol. Chem.* **281**, 5821–5828.
Storoni, L. C., McCoy, A. J. & Read, R. J. (2004). *Acta Cryst.* D**60**, 432–438.
Sturm, A., Amino, R., van de Sand, C., Regen, T., Retzlaff, S., Rennenberg, A., Krueger, A., Pollok, J. M., Menard, R. & Heussler, V. T. (2006). *Science*, **313**, 1287–1290.
Trakhanov, S., Kreimer, D. I., Parkin, S., Ames, G. F. & Rupp, B. (1998). *Protein Sci.* **7**, 600–604.
Trakhanov, S. & Quiocho, F. A. (1995). *Protein Sci.* **4**, 1914–1919.
Wang, S. X., Pandey, K. C., Scharfstein, J., Whisstock, J., Huang, R. K., Jacobelli, J., Fletterick, R. J., Rosenthal, P. J., Abrahamson, M., Brinen, L. S., Rossi, A., Sali, A. & McKerrow, J. H. (2007). *Structure*, **15**, 535–543.
Wang, S. X., Pandey, K. C., Somoza, J. R., Sijwali, P. S., Kortemme, T., Brinen, L. S., Fletterick, R. J., Rosenthal, P. J. & McKerrow, J. H. (2006). *Proc. Natl Acad. Sci. USA*, **103**, 11503–11508.
Weiss, M. S. & Hilgenfeld, R. (1997). *J. Appl. Cryst.* **30**, 203–205.